

Communication: Isotopic effects on tunneling motions in the water trimer

Pablo E. Videla, Peter J. Rossky, and D. Laria

Citation: The Journal of Chemical Physics **144**, 061101 (2016); doi: 10.1063/1.4941701
View online: http://dx.doi.org/10.1063/1.4941701
View Table of Contents: http://scitation.aip.org/content/aip/journal/jcp/144/6?ver=pdfcov
Published by the AIP Publishing

Articles you may be interested in

An ab initio study of tunneling splittings in the water trimer
J. Chem. Phys. **123**, 044302 (2005); 10.1063/1.1954768

Bifurcation tunneling dynamics in the water trimer
J. Chem. Phys. **117**, 8823 (2002); 10.1063/1.1509750

Tunneling splittings in water trimer by projector Monte Carlo
J. Chem. Phys. **112**, 2218 (2000); 10.1063/1.480788

Rearrangements and tunneling splittings of protonated water trimer
J. Chem. Phys. **111**, 8429 (1999); 10.1063/1.480183

Pseudorotation tunneling in several water trimer isotopomers
J. Chem. Phys. **110**, 823 (1999); 10.1063/1.478050



Reuse of AIP Publishing content is subject to the terms: https://publishing.aip.org/authors/rights-and-permissions. Downloaded to IP: 67.189.219.1 On: Sun, 07 Aug 2016 21:34:52

Communication: Isotopic effects on tunneling motions in the water trimer

Pablo E. Videla,[1] Peter J. Rossky,[2] and D. Laria[1,3,a)]
[1]*Departamento de Química Inorgánica Analítica y Química-Física e INQUIMAE, Facultad de Ciencias Exactas y Naturales, Universidad de Buenos Aires, Ciudad Universitaria, Pabellón II, 1428 Buenos Aires, Argentina*
[2]*Department of Chemistry, Rice University, Houston, Texas 77251-1892, USA*
[3]*Departamento de Física de la Materia Condensada, Comisión Nacional de Energía Atómica, Avenida Libertador 8250, 1429 Buenos Aires, Argentina*

(Received 6 January 2016; accepted 28 January 2016; published online 8 February 2016)

We present results of ring polymer molecular dynamics simulations that shed light on the effects of nuclear quantum fluctuations on tunneling motions in cyclic $[H_2O]_3$ and $[D_2O]_3$, at the representative temperature of $T = 75$ K. In particular, we focus attention on free energies associated with two key isomerization processes: The first one corresponds to flipping transitions of dangling OH bonds, between up and down positions with respect to the O–O–O plane of the cluster; the second involves the interchange between connecting and dangling hydrogen bond character of the H-atoms in a tagged water molecule. Zero point energy and tunneling effects lead to sensible reductions of the free energy barriers. Due to the lighter nature of the H nuclei, these modifications are more marked in $[H_2O]_3$ than in $[D_2O]_3$. Estimates of the characteristic time scales describing the flipping transitions are consistent with those predicted based on standard transition-state-approximation arguments. © *2016 AIP Publishing LLC*. [http://dx.doi.org/10.1063/1.4941701]

The water trimer represents a singular, attractive aggregate for study among the symmetric aqueous nanoclusters comprising less than ten molecules.[1] Structurally speaking, the overall shape of $[H_2O]_3$ can be cast in terms of a cyclic, quasiplanar ring arrangement, in which water molecules are bound by three strained (non-linear) H-bonds, articulated via connective ("c") hydrogens H^c. Moreover, the O–O–O plane determines up ("u") and down ("d") locations for the remaining three free ("f") hydrogens H^f, in terms of their out-of-plane (OOP) positions (see Fig. 1(a)). Provided the connective characteristics of the individual H-atoms are preserved, global minimum structures of the water trimer include six equivalent $[uud], [udu], [duu], [ddu], [dud], [udd]$, OOP isomers.

The analysis of the water trimer is particularly enlightening since it represents the simplest aqueous cluster whose collective motions have already incorporated basic elements that control H-bond dynamics in more complex, bulk environments. The characteristics of libration and intramolecular vibrational modes in liquid water turn out to be insensitive to the local architecture of the intermolecular connectivity prevailing in the vicinity of molecules undergoing ruptures and subsequent reconstructions of H-bonds.[2]

There is a wealth of experimental and theoretical evidence confirming that interconversions between the manifold of minimum energy structures in $[H_2O]_3$ are controlled by two main tunneling motions.[1,3–30] The first one,

$$H^cOH^f_d \rightarrow H^cOH^f_u, \tag{1}$$

corresponds to rotations of free hydrogens around O–H^c intramolecular bonds, flipping their positions from one side of the oxygen plane to the other one (see Fig. 1(a)). In addition, interconversions between different minima can proceed via bifurcation pathways (see Fig. 1(b)), along which there is an interchange between free and connecting character of the two hydrogen atoms (H_1 and H_2) in a tagged donor-water molecule hydrogen bonded to an acceptor ("a") molecule,

$$H^f_1O_dH^c_2\cdots O_a \rightarrow H^f_2O_dH^c_1\cdots O_a. \tag{2}$$

In what follows, we will present results from ring-polymer-molecular-dynamics[31,32] (RPMD) simulations that describe the magnitude of nuclear quantum effects on the dynamical characteristics of these two tunneling processes at a nominal temperature of $T = 75$ K. The methodology relies on the path-integral representation of quantum statistical mechanics, which establishes a correspondence between the quantum system and a classical one comprised of a collection of interacting cyclic polymers, each with P molecular replicas.[33] For equilibrium quantities, RPMD can provide essentially exact quantum results, as does standard path integral molecular dynamics.[34] In addition, the methodology provides reasonable quantum mechanical estimates for characteristic time scales via the computation of appropriate RPMD time correlation functions. In order to capture the essential elements of the structure of these clusters, interparticle interactions were modeled using the *MB-pol* model, recently developed by Paesani and collaborators.[35–37] Following a similar spirit, Bowman and collaborators have developed an alternative potential that has also been successfully implemented in the dynamical analysis of predissociation channels for the water trimer following vibrational excitation of the stretching of the

a)Author to whom correspondence should be addressed. Electronic mail: dhlaria@cnea.gov.ar

 © 2016 AIP Publishing LLC

Reuse of AIP Publishing content is subject to the terms: https://publishing.aip.org/authors/rights-and-permissions. Downloaded to IP: 67.189.219.1 On: Sun, 07 Aug 2016 21:34:52

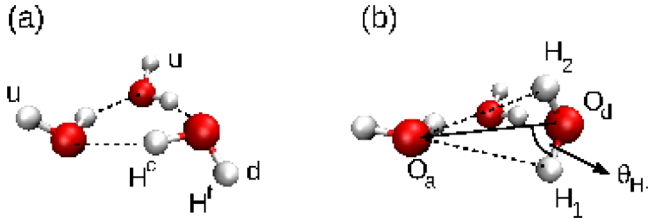


FIG. 1. $[H_2O]_3$. (a) $[uud]$ structure. (b) Transition-state configuration for the bifurcation isomerization.

OH bond.[30] A detailed description of the methodology, its implementation, and the quality of the *MB-pol*[37] model predictions for geometrical parameters corresponding to the potential energy minima of the water trimer are provided as the supplementary material.[38]

To move forward in the characterization of the two isomerization channels described in Eqs. (1) and (2), it will be useful to first define microscopic order parameters that clearly distinguish reactant from product stable states. Our choices are the natural ones, based on geometric characteristics of the six low-lying stationary points of the water trimer reported in Ref. 39. For the flipping process, we found it convenient to define ξ^{flp} according to

$$\xi^{flp} = \frac{\mathbf{r}_{H^fO} \cdot \mathbf{r}^{\perp}}{|\mathbf{r}_{H^fO}|}, \tag{3}$$

where, in the previous equation, $\mathbf{r}_{\alpha\gamma} = \mathbf{r}_\alpha - \mathbf{r}_\gamma$ and $\mathbf{r}_\alpha$ denotes the position of the α nucleus in the tagged water molecule undergoing rotation, whereas $\mathbf{r}^{\perp}$ represents a unit vector perpendicular to O–O–O plane. Clearly, ξ^{flp} changes sign as a tagged, dangling H moves from one side of the O–O–O plane to the opposite, while $\xi \sim 0$ would identify transition-state-like configurations, with $\mathbf{r}_{H^fO}$ in the O–O–O plane. On the other hand, the interchange between free and connective characters shown in Eq. (2) can be described in terms of another order parameter ξ^{bif} defined as

$$\xi^{bif} = \theta_{H_2} - \theta_{H_1}, \tag{4}$$

with

$$\cos\theta_{H_i} = \frac{\mathbf{r}_{H_iO^d} \cdot \mathbf{r}_{O^aO^d}}{|\mathbf{r}_{H_iO^d}|\,|\mathbf{r}_{O^aO^d}|}. \tag{5}$$

The previous definition establishes a clear correspondence between positive (negative) values of ξ^{bif} and configurations in which $H_1(H_2)$ exhibits connective characteristics (see Fig. 1(b)).

Armed with the latter definitions, one can compute associated free energy profiles, $A(\xi)$, of the type

$$\beta A(\xi') \propto -\ln\langle\delta(\xi - \xi')\rangle, \tag{6}$$

where $\langle\cdots\rangle$ denotes an equilibrium ensemble average and $\delta(x)$ is the Dirac delta function. Normally, within a path-integral framework, two alternatives are available to compute the previous expression: the first one establishes a natural correspondence between nuclear positions $\mathbf{r}_\alpha$ and centroid coordinates[40–42] of the isomorphic ring polymers, leading to centroid free energies of the type

$$\beta A(\xi') \propto -\ln\langle\delta(\xi(\{\mathbf{r}_N^{cnt}\}) - \xi')\rangle, \tag{7}$$

where

$$\mathbf{r}_\alpha^{cnt} = \frac{1}{P}\sum_{k=1}^{P}\mathbf{r}_\alpha^{(k)}, \tag{8}$$

and in the previous equation, $\mathbf{r}_\alpha^{(k)}$ is the position of particle α at the imaginary time slice k. As such, centroid free energies are obtained by collecting statistics for the order parameters, evaluated in terms of particles centroids, in a classical-like fashion. The second, more rigorous, route involves the following "bead average" computation, namely,

$$\begin{aligned}\beta A(\xi') &\propto -\ln\langle\delta(\xi(\{\mathbf{r}_N\}) - \xi')\rangle \\ &= -\ln\left[\frac{1}{P}\sum_{k=1}^{P}\langle\delta(\xi(\{\mathbf{r}_N^{(k)}\}) - \xi')\rangle\right].\end{aligned} \tag{9}$$

From a quantitative perspective, the energetics of the two isomerization channels differ in a sensible fashion. Note that the bifurcation route requires the partial rupture and subsequent reconstruction of a H-bond, a process that, in the gas phase, involves energies typically ~2 kcal mol^{-1}.[1] Consequently, at temperatures of the order of, or below say, $T \sim 100$ K, these episodes can be regarded as rare events. On the other hand, flipping episodes are articulated by rotations of non-connecting atoms and involve surmounting much lower energy barriers that barely surpass a few tenths of kcal mol^{-1}. In fact, in the course of all trajectories obtained in this work — lasting ~2 ns — we found no evidence of spontaneous bifurcation events whereas flipping episodes were sufficiently frequent to allow us to harvest meaningful statistics along standard equilibrium trajectories.

Classical and quantum profiles for centroid free energies associated to flipping isomerizations in $[H_2O]_3$ and $[D_2O]_3$ at $T = 75$ K are presented in Fig. 2(a). The classical profile presents two minima at $|\xi| \sim 0.75$, separated by a $\sim 2k_BT$

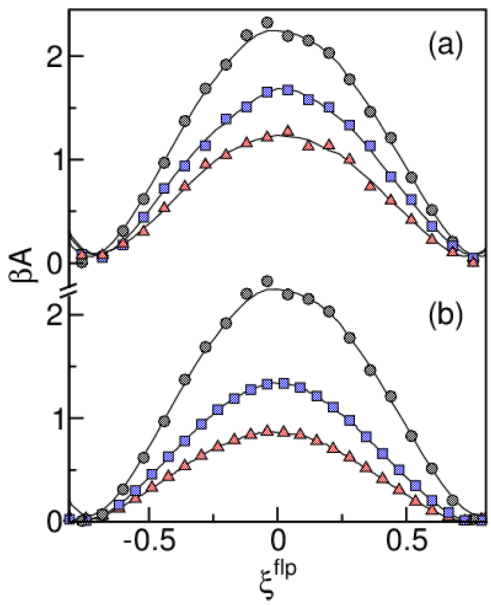


FIG. 2. Free energy associated with the flipping of a dangling H from one side of the trimer plane to the other, obtained from (a) centroid and (b) "bead" samplings (see text). Classical $[H_2O]_3$ (black circles), quantum $[D_2O]_3$ (red squares), and quantum $[H_2O]_3$ (blue triangles).

Reuse of AIP Publishing content is subject to the terms: https://publishing.aip.org/authors/rights-and-permissions. Downloaded to IP: 67.189.219.1 On: Sun, 07 Aug 2016 21:34:52

barrier located at $\xi = 0 = \xi^{\dagger}$. While the locations of the corresponding minima are practically unchanged for classical and quantum cases, the magnitudes of the free energy barriers strongly depend on the masses of the light particles. In agreement with previous simulations results,[41] combined effects from zero point energy (ZPE) and tunneling lead to a sensible ~20% reduction for $[D_2O]_3$; moreover, for $[H_2O]_3$ isotopomers, the reduction in the activation energy is more pronounced, about ~50% from the classical value. The profiles in the lower part of Fig. 2, corresponding to "bead averages" (see Eq. (9)), reveal even more marked modifications; the incorporation of quantum fluctuations brings the magnitudes of barriers down to 60% and 40% of the classical estimate for $[D_2O]_3$ and $[H_2O]_3$, respectively.

The differences in the results from the two sampling procedures are not totally unexpected given the highly non-linear nature of the order parameter with respect to the particle coordinates. Note that, in performing classical-like centroid sampling, effects from quantum fluctuations arising from the spatial delocalization of the light particles are partially lost as one collects statistics restricted to mean values of particle positions. In contrast, at a fixed centroid configuration, "bead sampling" explicitly explores a wider spectrum of order parameters. These differences should be amplified in the less confining vicinity of transition-state-like states, where one expects more elongated H quantum distributions, stretching out laterally from reactant to product states.

A more vivid picture of the latter feature can be obtained by examining the profiles shown in Fig. 3(a), where we present estimates for the spatial extents of free protons along the flipping process. The results correspond to conditional probabilities of the type

$$\langle O(\xi')\rangle = \frac{\langle O(\{\mathbf{r}_N^{(k)}\})\,\delta(\xi-\xi')\rangle}{\langle \delta(\xi-\xi')\rangle}, \tag{10}$$

for $O = \mathcal{R}^2$, $\mathcal{R}^2_{\parallel}$, and $\mathcal{R}^2_{\perp}$. The first observable $\mathcal{R}^2$ represents the imaginary time mean square displacement of the proton and provides an estimate for its spatial delocalization;[43,44] on the other hand, $\mathcal{R}^2_{\perp}$ and $\mathcal{R}^2_{\parallel}$ denote the corresponding decompositions into perpendicular and parallel projections along directions with respect to the O–H bonds, namely, $\mathcal{R}^2 = \mathcal{R}^2_{\parallel} + 2\mathcal{R}^2_{\perp}$.[45–47]

The fact that $\mathcal{R}_{\perp}$ looks longer than $\mathcal{R}_{\parallel}$ — which, incidentally, remains practically unchanged along the reactive pathway — is the consequence of combined effects from the local intra- and intermolecular interactions and leads to distributions resembling prolate ellipsoids.[44] This interplay is also responsible for the larger spatial delocalization that the flipping hydrogens show at the vicinity of transition states, $\mathcal{R}_{\perp}(\xi^{\dagger}) \sim 0.34$ Å, compared to stable reactant/product states, where $\mathcal{R}_{\perp}(\xi^{flp} = \pm 0.75) \sim 0.30$ Å. Interestingly, the latter lengthscales are of similar order to the displacements covered by the proton to reach transition states, $\delta\ell \sim 0.75$ Å, a fact that alone would imply important tunneling effects in the free energy barrier.

In Fig. 4, we present plots for free energies associated with bifurcation events. As mentioned, the energy barrier is intrinsically higher in this case and required the use of a biased-sampling technique; we used a standard umbrella sampling strategy.[38,48] At a first sight, the plots reveal that the incorporation of quantum fluctuations leads to much milder modifications in the profiles, compared to classical scenarios. For $[H_2O]_3$, the ratio between quantum and classical centroid free energy barriers for the bifurcation process was found to be $A^{qntm}(\xi^{\dagger})/A^{clss}(\xi^{\dagger}) \sim 0.85$ whereas, for "bead sampling," the ratio moved down to ~0.70. The fact that classical and quantum calculations look more comparable is, in part, expected given the more marked disparity between the magnitudes of the energetic barrier and the zero point energy of the trimer.

However, a closer examination shows that the absolute magnitude of the quantum effect expressed in terms of

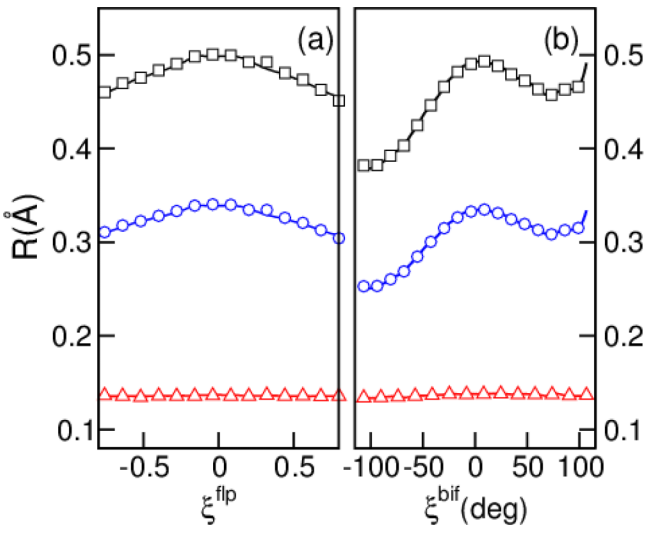


FIG. 3. (a) Correlation lengths for the proton isomorphic polymers along flipping transitions (H^f to H^f identities) in $[H_2O]_3$. (b) Correlation lengths for the isomorphic polymer associated to atom H_2 (see Fig. 1(b)), along the bifurcation pathway taking H_2 from H^c to H^f identities (see text). $\mathcal{R}$: black, open squares; $\mathcal{R}_{\perp}$: blue, open circles; $\mathcal{R}_{\parallel}$: red, open triangles.

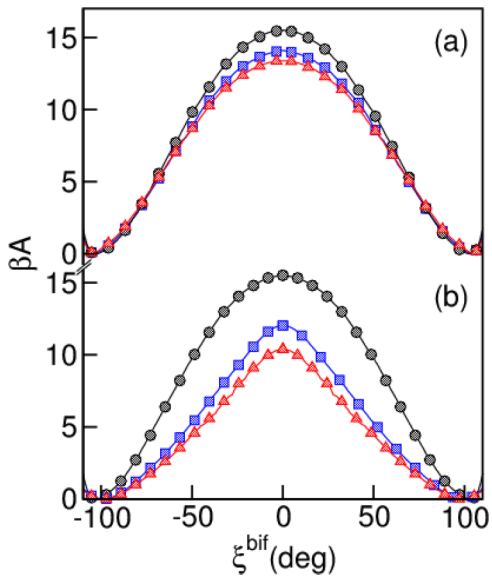


FIG. 4. Free energy associated with bifurcation transitions. Same labeling as Fig. 2.

Reuse of AIP Publishing content is subject to the terms: https://publishing.aip.org/authors/rights-and-permissions. Downloaded to IP: 67.189.219.1 On: Sun, 07 Aug 2016 21:34:52

TABLE I. Characteristic time scales for flipping isomerizations.

	τ_{flp}^{cl} (ps)	τ_{flp}^{qntm} (ps)	$\tau_{flp}^{cl}/\tau_{flp}^{qntm}$	$e^{-\beta\Delta A_{flp}^{\dagger}}$	$e^{-\beta\Delta A_{bif}^{\dagger}}$
H_2O	0.61	0.21	2.9	2.7[a](4.0[b])	9.1[a](~200[b])
D_2O	0.76	0.42	1.8	1.7[a](2.4[b])	4.6[a](~40[b])

[a]Centroid sampling.
[b]"Bead" sampling.

$\Delta A^{\dagger} = A^{qntm}(\xi^{\dagger}) - A^{clss}(\xi^{\dagger})$ is enhanced in the bifurcation process (see entries in the last two columns, on the right hand side part of Table I). This case involves a reversal of identity of each H, between connected (H^c) and free (H^f), so that the change in the degree of quantum delocalization from reactant to transition state to product is much larger along this pathway (see Fig. 3(b)). Correspondingly, the incremental quantum effect on $A(\xi^{\dagger})$ is larger. Equivalently, the rate of the processes would be relatively more impacted by quantum effects for the bifurcated transition state, albeit a far slow process than the flipping route.

We will close our analysis with a brief comment on dynamical aspects related to flipping isomerization processes. Assuming that such interconversions can be described in terms of a first-order kinetic model, the RPMD-characteristic time scale τ_{flp} can be extracted from the time integrals of the normalized time correlation functions $C_{flp}^{\mathrm{RPMD}}(t)$,[38,49,50]

$$\tau_{flp}^{\mathrm{RPMD}} \sim \int_0^{\infty} C_{flp}^{\mathrm{RPMD}}(t)\, \mathrm{d}t, \tag{11}$$

where

$$C_{flp}^{\mathrm{RPMD}}(t) = \frac{\langle \delta h[\{\xi_i(t)\}] \cdot \delta h[\{\xi_i(0)\}] \rangle}{\langle (\delta h)^2 \rangle}, \tag{12}$$

with $\delta h = h - \langle h \rangle$. In the previous equation, $h[\{\xi_i(t)\}]$ represents a microscopic characteristic function that depends on the instantaneous set of order parameters $\{\xi_i^{flp}(t)\}$ $(i = 1,2,3)$, defined in terms of centroid coordinates. Following previous studies,[51] we adopted the "first-passage" or "continuum" definition for the characteristic function. As such, $h(t)$ equals unity if, along the $[0,t]$ time interval, the cluster exhibits continuously one tagged OOP minimum energy configuration — arbitrarily chosen out of the six available — and zero otherwise.

In Fig. 5, we present results of classical and quantum $C_{flp}^{\mathrm{RPMD}}(t)$ for $[H_2O]_3$ and $[D_2O]_3$, whereas the results for the corresponding time integrals are listed in Table I. The inset in the figure shows that all curves exhibit single exponential decays after initial ~1 ps transients. The values of τ_{flp}^{qntm} are between two and three times smaller than τ_{flp}^{clss}, with the difference much more marked for the light water case. Interestingly, inspection of the third and fourth columns in Table I reveals that for both clusters, $[H_2O]_3$ and $[D_2O]_3$, the ratios between quantum and classical τ_{flp} follow closely the ones predicted by the sole consideration of the differences in the magnitudes of the corresponding centroid free energy barriers. This observation brings additional consistency to our calculations, given the fact that the first passage criterion used in evaluating the dynamical rate follows closely the spirit of the transition state approximation, which neglects

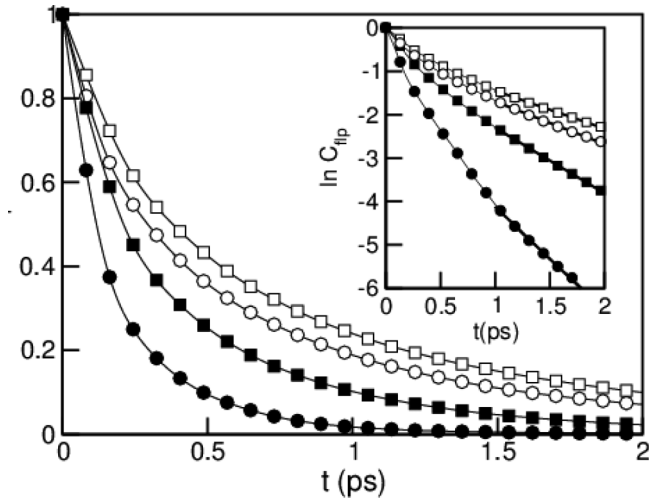


FIG. 5. RPMD time correlation function for flipping transitions in aqueous trimers. $[H_2O]_3$: circles; $[D_2O]_3$: squares. Classical results: open symbols; quantum estimates: solid symbols. The thick solid lines in the inset represent linear regressions for $t \geq 1$ ps.

contributions to the rates from trajectories exhibiting multiple recrossings over free energy barriers.[50]

The main conclusions of this study can be summarized as follows: (i) the present contribution represents the first quantum dynamics study related to the two main tunneling motions with sufficient sampling to yield actual estimates for rates, using a potential that is demonstrably accurate in its structural predictions. Incidentally, one can anticipate that the results should not differ considerably if they were computed using the WHBB alternative model;[30,39] (ii) our simulation results show that, in the water trimer at moderately low temperatures (~75 K), the explicit incorporation of nuclear quantum fluctuations leads to sensible significant reductions in the free energy barriers associated with flipping and bifurcation isomerization channels; (iii) the relative rate enhancement for the latter route is larger since there is a greater increase in proton delocalization in the bifurcated structure relative to the connected geometry (a hydrogen bond is partially broken). However, the overall rate for this route is, in any case, much lower than that for flipping for the same reason. For the latter pathway, the magnitude of the barrier is comparable to the variation in the ZPE of the cluster along the reaction coordinate, leading to reductions in the observed characteristic time scale describing transitions by factors of ~2 for $[D_2O]_3$ and of ~3 for $[H_2O]_3$. Moreover, these rates seem to follow those predicted via the consideration of simple standard transition-state-theory arguments.

We are grateful to Professor F. Paesani for very helpful discussions regarding the predictive capacity of water potentials. D.L. is a staff member of CONICET (Argentina). P.J.R. acknowledges the support of the U.S. National Science Foundation (No. CHE-1362381).

[1]F. N. Keutsch, J. D. Cruzan, and R. J. Saykally, Chem. Rev. **103**, 2533 (2003).
[2]A. Luzar and D. Chandler, Phys. Rev. Lett. **76**, 928 (1996).
[3]N. Pugliano and R. J. Saykally, Science **257**, 1937 (1992).
[4]M. Schutz, T. Burgi, S. Leutwyler, and H. B. Burgi, J. Chem. Phys. **99**, 5228 (1993).

Reuse of AIP Publishing content is subject to the terms: https://publishing.aip.org/authors/rights-and-permissions. Downloaded to IP: 67.189.219.1 On: Sun, 07 Aug 2016 21:34:52

[5]D. J. Wales, J. Am. Chem. Soc. **115**, 11180 (1993).
[6]D. J. Wales, J. Am. Chem. Soc. **115**, 11191 (1993).
[7]K. Liu *et al.*, J. Am. Chem. Soc. **116**, 3507 (1994).
[8]S. Suzuki and G. A. Blake, Chem. Phys. Lett. **229**, 499 (1994).
[9]K. Liu *et al.*, Faraday Discuss. **97**, 35 (1994).
[10]J. G. C. M. van Duijneveldt-van de Rijdt and F. B. van Duijneveldt, Chem. Phys. Lett. **237**, 560 (1995).
[11]T. Burgi, S. Graf, S. Leutwyler, and W. Klopper, J. Chem. Phys. **103**, 1077 (1995).
[12]J. K. Gregory and D. C. Clary, J. Chem. Phys. **102**, 7817 (1995).
[13]K. Liu, M. G. Brown, M. R. Viant, J. D. Cruzan, and R. Saykally, Mol. Phys. **89**, 1373 (1996).
[14]A. van der Avoird, E. H. T. Olthof, and P. E. S. Wormer, J. Chem. Phys. **105**, 8034 (1996).
[15]T. R. Walsh and D. J. Wales, J. Chem. Soc., Faraday Trans. **92**, 2505 (1996).
[16]M. R. Viant *et al.*, J. Phys. Chem. A **101**, 9032 (1997).
[17]M. G. Brown *et al.*, J. Chem. Phys. **111**, 7789 (1999).
[18]D. Sabo, Z. Bacic, S. Graf, and S. Leutwyler, J. Chem. Phys. **111**, 10727 (1999).
[19]F. N. Keutsch, E. N. Karyakin, R. J. Saykally, and A. van der Avoird, J. Chem. Phys. **114**, 3988 (2001).
[20]F. N. Keutsch, R. S. Fellers, M. R. Viant, and R. J. Saykally, J. Chem. Phys. **114**, 4005 (2001).
[21]F. N. Keutsch *et al.*, J. Chem. Phys. **114**, 3994 (2001).
[22]T. Taketsugu and D. J. Wales, Mol. Phys. **100**, 2793 (2002).
[23]M. Mandziuk, J. Phys. Chem. A **108**, 121 (2004).
[24]D. V. Shalashilin, M. S. Child, and D. C. Clary, J. Chem. Phys. **120**, 5608 (2004).
[25]J. A. Anderson, K. Crager, L. Fedoroff, and G. S. Tschumper, J. Chem. Phys. **121**, 11023 (2004).
[26]M. Takahashi, Y. Watanabe, T. Taketsugu, and D. J. Wales, J. Chem. Phys. **123**, 044302 (2005).
[27]J.-x. Han *et al.*, Chem. Phys. Lett. **423**, 344 (2006).
[28]G. Czak, A. L. Kaledin, and J. M. Bowman, Chem. Phys. Lett. **500**, 217 (2010).
[29]J. O. Richardson, S. C. Althorpe, and D. J. Wales, J. Chem. Phys. **135**, 124109 (2011).
[30]L. C. Ch'ng, A. K. Samanta, Y. Wang, J. M. Bowman, and H. Reisler, J. Phys. Chem. A **117**, 7207 (2013).
[31]I. R. Craig and D. E. Manolopoulos, J. Chem. Phys. **121**, 3368 (2004).
[32]S. Habershon, D. E. Manolopoulos, T. E. Markland, and T. F. Miller III, Annu. Rev. Phys. Chem. **64**, 387 (2013).
[33]D. Chandler and P. Wolynes, J. Chem. Phys. **74**, 4078 (1981).
[34]M. E. Tuckerman, B. J. Berne, G. J. Martyna, and M. L. Klein, J. Chem. Phys. **99**, 2796 (1993).
[35]V. Babin, C. Leforestier, and F. Paesani, J. Chem. Theory Comput. **9**, 5395 (2013).
[36]V. Babin, G. R. Medders, and F. Paesani, J. Chem. Theory Comput. **10**, 1599 (2014).
[37]V. Babin, G. R. Medders, and F. Paesani, J. Chem. Theory Comput. **10**, 2906 (2014).
[38]See supplementary material at http://dx.doi.org/10.1063/1.4941701 for additional technical details and a brief discussion about the reliability of the dynamical predictions of the RPMD method.
[39]Y. Wang, B. Shepler, B. J. Braams, and J. M. Bowman, J. Chem. Phys. **131**, 54511 (2009).
[40]R. P. Feynman, *Statistical Mechanics* (Addison-Wesley, Reading, MA, 1972).
[41]J. Lobaugh and G. A. Voth, Chem. Phys. Lett. **198**, 311 (1992).
[42]J. Lobaugh and G. A. Voth, J. Chem. Phys. **100**, 3039 (1994).
[43]A. L. Nichols, D. Chandler, Y. Singh, and D. M. Richardson, J. Chem. Phys. **81**, 5109 (1984).
[44]P. E. Videla, P. J. Rossky, and D. Laria, J. Chem. Phys. **139**, 174315 (2013).
[45]T. E. Markland and B. J. Berne, Proc. Natl. Acad. Sci. U. S. A. **109**, 7988 (2012).
[46]J. Liu *et al.*, J. Phys. Chem. C **117**, 2944 (2013).
[47]P. E. Videla, P. J. Rossky, and D. Laria, J. Phys. Chem. Lett. **4**, 2375 (2014).
[48]D. Frenkel and B. Smit, *Understanding Molecular Simulation: From Algorithms to Applications* (Academic Press, 2001), Chap. 7.
[49]I. R. Craig and D. E. Manolopoulos, J. Chem. Phys. **122**, 084106 (2005).
[50]I. R. Craig and D. E. Manolopoulos, J. Chem. Phys. **123**, 034102 (2005).
[51]A. Luzar, J. Chem. Phys. **113**, 10663 (2000).

Reuse of AIP Publishing content is subject to the terms: https://publishing.aip.org/authors/rights-and-permissions. Downloaded to IP: 67.189.219.1 On: Sun, 07 Aug 2016 21:34:52